Universität Karlsruhe (TH)
Institut für Baustatik

A Finite Element Model
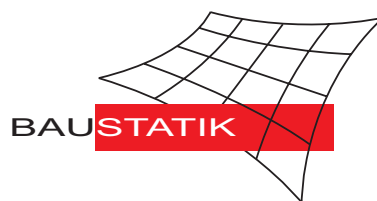# for the Analysis of Delaminations
in FRP–Shells

F. Gruttmann, W. Wagner

Mitteilung 7(2001)

BAUSTATIK

Universität Karlsruhe (TH)
Institut für Baustatik

A Finite Element Model
for the Analysis of Delaminations
in FRP–Shells

F. Gruttmann, W. Wagner

Mitteilung 7(2001)

BAUSTATIK

Prof. Dr.–Ing. W. Wagner
Institut für Baustatik
© Universität Karlsruhe
Postfach 6980
76128 Karlsruhe

Telefon: (0721) 608–2280
Telefax: (0721) 608–6015
E–mail: bs@.uni-karlsruhe.de
Internet: http://www.bs.uni-karlsruhe.de

A FINITE ELEMENT MODEL FOR THE ANALYSIS OF DELAMINATIONS IN FRP–SHELLS

Friedrich Gruttmann[*]

Institute for Structural Analysis
University of Darmstadt
D-64283 Darmstadt, Germany
e-mail: gruttmann@statik.tu-darmstadt.de
web page: www.st.bauing.tu-darmstadt.de

Werner Wagner

Institute for Structural Analysis
University of Karlsruhe(TH)
D-76131 Karlsruhe, Germany
Email: ww@bs.uni-karlsruhe.de
web page: www.uni-karlsruhe.de/~baustatik

Abstract. This paper presents a finite element method to simulate growing delaminations in composite structures. The delamination process, using an inelastic material law with softening, takes place within an interface layer having a small, but non–vanishing thickness. A stress criterion is used to detect the critical points. To prevent mesh dependent solutions a regularization technique is applied. The artificial viscosity leads to corresponding stiffness matrices which guarantee stable equilibrium iterations. The essential material parameter which describes the delamination process is the critical energy release rate. The finite element calculations document the robustness and effectivity of the developed model. Extensive parameter studies are performed to show the influence of the introduced geometrical and material quantities.

Key words: Composite laminates, delamination, viscoplasticity, finite elements.

1 INTRODUCTION

One of the most dangerous failure modes in composite laminates is delamination. The loss of strength and stiffness may reduce the lifetime in a significant way. To utilize the full potential of composites it is necessary to analyze initiation and growth of delamination which may be a basis of appropriate construction measures.

Due to the complexity of the underlying mathematical model, usually numerical procedures are applied to compute increasing delaminations. The so–called first–ply failure analysis yields the location where damage starts. Several authors use stress–based criteria to predict different failure modes. If the criterion is not fulfilled stiffness parameters are reduced or set to zero. The procedure may not work if the stress field is singular. Another disadvantage is a lack of robustness within the equilibrium iterations. This holds especially for geometrical nonlinear calculations.

Other authors use a fracture mechanics approach. When the energy related to the newly opened crack-surface exceeds a critical value, the crack extends. In so-called virtual crack-extension or crack-closure methods the energy release rate is calculated

using the nodal forces and displacements within the finite element method, see e.g. Wang et.al.[1] A considerable number of iterations may be necessary until a configuration is found where equilibrium and delamination criterion are fulfilled.

In some papers interface elements with double nodes are used to map the geometric discontinuities arising within the delamination process. Schellekens and de Borst[2] developed plane strain elements and associated interface elements with cubic interpolation functions. Crisfield[3] modified the concept along with eight–node quadrilateral plane strain elements. In their approach the constitutive equations are formulated directly in terms of crack opening displacements.

The goal of this paper is to present an effective finite element tool for the numerical analysis of delaminations in layered composites. The essential features and novel aspects are summarized as follows.

To account for the three–dimensional stress state, which typically occurs in composite structures, the discretization is performed using hexahedral elements. Due to special interpolation techniques based on mixed variational principles the elements are able to predict the stress state even for very thin structures. Applying an assumed strain method (ANS), the transverse shear strains are independently interpolated, see e.g. Bathe and Dvorkin.[5] Furthermore, the thickness strains are approximated according to the paper of Betsch and Stein.[6] The membrane behaviour is improved by applying the enhanced assumed strain method (EAS) with five parameters. The variational formulation and detailed finite element equations of the ANS–EAS5–element are given in Klinkel, Gruttmann and Wagner.[4]

Delamination of layered composites usually occurs together with damage within the plies. The complicated interaction between the different failure modes is not considered in the paper. Within the present model delamination takes place in interface layers with small but not vanishing thickness. The interlaminar stresses are determined using an inelastic material law with softening. The slope of the softening curve is determined by the critical energy release rate, the thickness of the interface layer and the tensile strength of the laminate in thickness direction. Complete delamination is defined if the newly opened surface is free of stresses. To avoid mesh dependent solutions a regularization technique is applied.

2 DELAMINATION MODEL

2.1 Interface layer

Fig. 1 shows a finite element discretization of a plate strip using eight–node elements. The interface layers, with thickness h_t, are positioned in those regions where delamination is expected. Our numerical investigations showed that the behaviour of the global composite structure remains practically unaltered for thickness ratios of $h_t/h \leq 10^{-2}$, where h denotes the thickness of the total laminate, see Fig. 2. Using a material formulation, the variational equations are written in terms of the Second Piola–Kirchhoff stress tensor $\mathbf{S}$ and the work conjugate Green–Lagrangian strain tensor $\mathbf{E}$. The tensor components refer to different basis systems, where the transformations are specified in Sprenger, Gruttmann and Wagner.[7]

In this paper the criterion of Hashin[8] in terms of the interlaminar normal stresses S^{33} and shear stresses S^{13} and S^{23} is used to predict the location where delamination occurs. Introducing a local Cartesian coordinate system one obtains
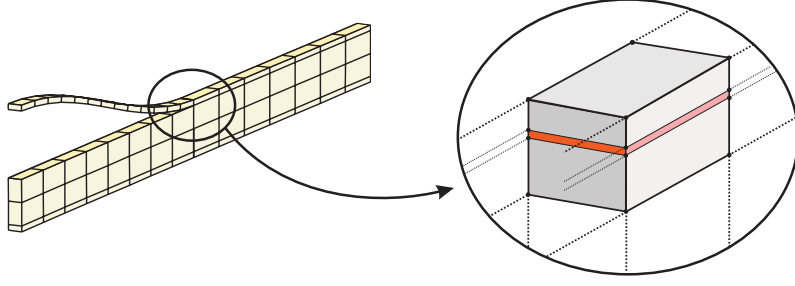
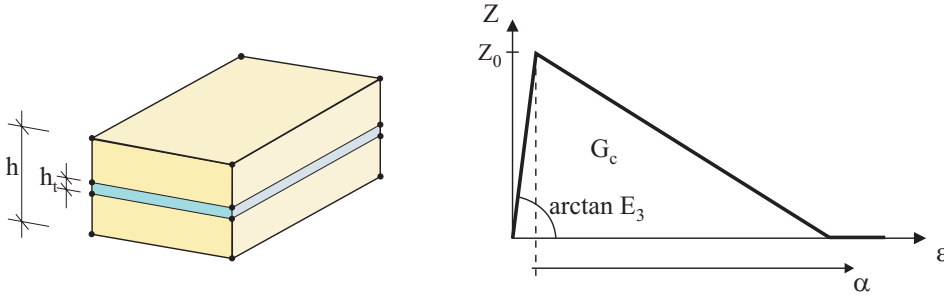Figure 1: Plate strip with delaminated layer and interface element

Figure 2: Interface layer and softening function

$$\frac{(S^{33})^2}{Z_0^2} + \frac{(S^{13})^2 + (S^{23})^2}{R_0^2} \leq 1 \,. \tag{1}$$

Here, Z_0 and R_0 denote the tensile strength in thickness direction and the shear strength of the laminate, respectively. The criterion can only be formulated in terms of Second Piola Kirchhoff stresses, if the application is restricted to small deformations. Otherwise the transformation to the Cauchy stress tensor $\boldsymbol{\sigma}$ has to be considered.

Furthermore, linear softening behaviour according to Fig. 2 is introduced

$$Z(\alpha) = Z_0 \, (1 - \mu\alpha) \geq 0 \qquad \text{with} \ \ \mu > 0 \,, \tag{2}$$

where the internal variable α denotes the equivalent inelastic strain. The critical energy release G_c rate corresponds to the area under the softening curve multiplied with h_t, since in the present model the energy is dissipated within the interface layer of thickness h_t, thus

$$G_c = \frac{Z_0^2 h_t}{2} \, (\frac{1}{E_3} + \frac{1}{Z_0 \mu}) \,, \tag{3}$$

where E_3 denotes the elastic modulus in thickness direction. If the elastic deformations are negligible, which means that the first term in the sum cancels out, the softening parameter μ can easily be determined from (3) as

$$\mu \ = \ \frac{Z_0 \, h_t}{2 \, G_c} \,. \tag{4}$$

Delamination is defined, when the absolute value of the interlaminar stress vector vanishes.

2.2 The rate–independent plasticity model

With the assumption of small strains the Green–Lagrange strain tensor $\mathbf{E}$ and the associated rate can be additively decomposed in an elastic and an inelastic part. The elastic part follows from the linear constitutive law. The inelastic strain rates and the evolution law for the equivalent plastic strains are given with the inelastic multiplier $\dot{\lambda}$. Summarizing, the rate–independent plasticity model is written as

$$
\begin{aligned}
\dot{\mathbf{E}} &= \dot{\mathbf{E}}^{el} + \dot{\mathbf{E}}^{in} , \\
\dot{\mathbf{E}}^{el} &= \mathbf{C}^{-1} \dot{\mathbf{S}} , \\
\dot{\mathbf{E}}^{in} &= \dot{\mathbf{E}}^{pl} = \dot{\lambda} \mathbf{N} , \\
\dot{\alpha} &= \dot{\lambda} .
\end{aligned}
\tag{5}
$$

The constitutive tensor $\mathbf{C}$ in terms of the elasticity constants E_i, G_{ij} and ν_{ij} is described in Sprenger, Gruttmann and Wagner.[7] Furthermore, $\mathbf{N}$ denotes the gradient of the yield function $F(\mathbf{S}, \alpha)$. The fracture criterion (1) is reformulated and extended by the softening function (2) as follows

$$
F(\mathbf{S}, \alpha) = g(\mathbf{S}) - Z(\alpha)
\tag{6}
$$

with

$$
g(\mathbf{S}) = \sqrt{\mathbf{S} \cdot \mathbf{A} \mathbf{S}} , \qquad \mathbf{A} = \mathrm{Diag}\left[0,\ 0,\ 1,\ 0,\ \left(\frac{Z_0}{R_0}\right)^2,\ \left(\frac{Z_0}{R_0}\right)^2 \right] .
\tag{7}
$$

The components of $\mathbf{A}$ refer to a local Cartesian coordinate system. For $\alpha = 0$ eq. (6) is another representation of (1). The loading–unloading conditions must hold

$$
\dot{\lambda} \geq 0 , \quad F \leq 0 , \quad \dot{\lambda} F = 0 .
\tag{8}
$$

In case of loading with $\dot{\lambda} > 0$ the rate equations (5) considering $\mathbf{N} = \mathbf{A} \mathbf{S} / g$ are approximately time–integrated using a backward Euler integration algorithm. Within a time step $t_{n+1} = t_n + \Delta t$ one obtains, after some algebraic manipulations, the stress tensor and the parameter α

$$
\begin{aligned}
\mathbf{S}_{n+1} &= \left[\mathbf{C}^{-1} + \frac{\lambda}{Z(\alpha_{n+1})} \mathbf{A} \right]^{-1} \left[\mathbf{E}_{n+1} - \mathbf{E}_n^{pl} \right] = \mathbf{P}\,\mathbf{E}^{tr} , \\
\alpha_{n+1} &= \alpha_n + \lambda .
\end{aligned}
\tag{9}
$$

Here, the notation $\lambda := \Delta t \dot{\lambda}_{n+1}$, $\mathbf{S}_{n+1} = \mathbf{S}(t_{n+1})$ and $\alpha_{n+1} = \alpha(t_{n+1})$ is used.

The linearization of the stress tensor yields the consistent tangent operator

$$
\bar{\mathbf{D}} = \mathbf{P} - \frac{\mathbf{P}\mathbf{N} \otimes \mathbf{P}\mathbf{N}}{\mathbf{N} \cdot \mathbf{P}\mathbf{N} + H} \quad , \qquad H = \frac{Z'}{1 - \lambda \frac{Z'}{Z}} ,
\tag{10}
$$

with $Z' := \mathrm{d}Z/\mathrm{d}\alpha$. If for $Z > 0$ the softening parameter μ increases certain values, negative diagonal terms in $\bar{\mathbf{D}}$ occur. In this case the global iteration process to solve the equilibrium equations becomes unstable. For $Z = 0$ the expressions for $\mathbf{P}$ and H are undefined. This can be avoided introducing a tolerance.

2.3 Viscoplastic regularization

To prevent the described numerical instabilities, we use a viscoplastic regularization technique. The strain rates are introduced according to the approach of Duvaut and Lions[9]

$$
\begin{aligned}
\dot{\mathbf{E}}^{in} &= \dot{\mathbf{E}}^{vp} = \frac{1}{\eta}\mathbf{C}^{-1}\left(\mathbf{S} - \bar{\mathbf{S}}\right), \\
\dot{\alpha} &= -\frac{1}{\eta}\left(\alpha - \bar{\alpha}\right),
\end{aligned}
\tag{11}
$$

where η denotes the normalized viscosity parameter. In the present case η is a purely numerical parameter which has the meaning of a relaxation time. The stresses $\bar{\mathbf{S}}$ and equivalent plastic strains $\bar{\alpha}$ denote the solutions of the rate–independent theory.

Substitution of eq. $(5)_2$ and $(11)_1$ into eq. $(5)_1$ yields another representation of (11)

$$
\begin{aligned}
\dot{\mathbf{S}} + \frac{1}{\eta}\mathbf{S} &= \mathbf{C}\,\dot{\mathbf{E}} + \frac{1}{\eta}\bar{\mathbf{S}}, \\
\dot{\alpha} + \frac{1}{\eta}\alpha &= \frac{1}{\eta}\bar{\alpha}.
\end{aligned}
\tag{12}
$$

The solutions of the homogeneous differential equations are obtained analytically. The inhomogeneous part is solved approximately using a backward Euler integration algorithm. Introducing $\mathbf{S}_n = \mathbf{S}(t_n)$, $\delta = \Delta t/\eta$ and $\beta = \exp(-\delta)$ we end up with

$$
\begin{aligned}
\mathbf{S}_{n+1} &= \beta\,\mathbf{S}_n + (1-\beta)\,\bar{\mathbf{S}}_{n+1} + \frac{1-\beta}{\delta}\,\mathbf{C}\,\Delta\mathbf{E}, \\
\alpha_{n+1} &= \beta\,\alpha_n + (1-\beta)\,\bar{\alpha}_{n+1}.
\end{aligned}
\tag{13}
$$

The viscoplastic tangent matrix follows immediately with

$$
\mathbf{D} = \frac{d\mathbf{S}}{d\mathbf{E}} = \frac{1-\beta}{\delta}\,\mathbf{C} + (1-\beta)\,\bar{\mathbf{D}},
\tag{14}
$$

The first term in (14) leads to positive diagonal entries in the viscoplastic tangent matrix, where the factor δ implies that with decreasing η the time increment Δt has to be reduced, to obtain the desired effect. The symmetric matrix $\mathbf{D}$ is necessary to setup the tangent stiffness matrix for the equilibrium iteration.

3 EXAMPLES

3.1 Double cantilever beam test

As a the first example we investigate a double cantilever beam with a given initial delamination. The resultant load $q \cdot b$ amounts to 1.0 kN. We compare our numerical results with experimental investigations of Aliyu and Daniel.[10] The authors determined a critical energy release rate $G_c = 0.222\ N/mm$ using a crack opening velocity of $\dot{w} = 0.85\ mm/s$. The used material properties for an AS-4/3501-6 graphite epoxy are summarized in Fig. 3. The fiber direction within the whole structure corresponds to the global x–direction .

Due to the symmetry of the structure and loading conditions, only a quarter of the beam has to be discretized. We use two elements in y–direction and three elements in z–direction respectively. The number of elements $n_1 - n_4$ in x–direction can be seen in Fig. 3. The thickness of the interface layer is chosen as $h_t = h/100$. The energy release rate is the energy of a body with a certain volume referring to the newly opened delamination area. Since in the present case only the lower part of the beam

$$
\begin{aligned}
E_1 &= 138000 &&N/mm^2 \\
E_2 &= 8960 &&N/mm^2 \\
G_{12} &= 7100 &&N/mm^2 \\
G_{23} &= 3446 &&N/mm^2 \\
\nu_{12} &= 0.3 \\
Z_0 &= 51.7 &&N/mm^2 \\
R_0 &= 91.7 &&N/mm^2 \\
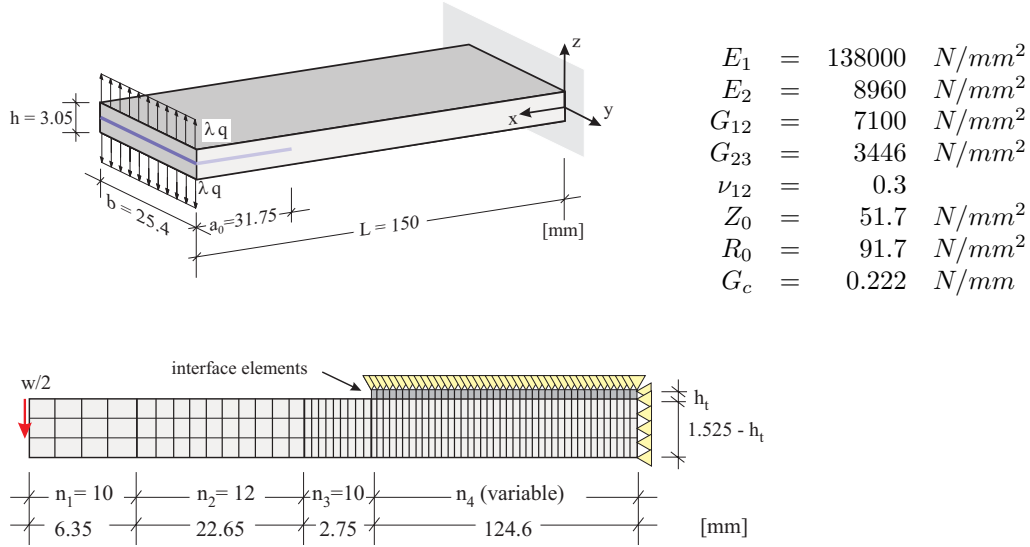G_c &= 0.222 &&N/mm
\end{aligned}
$$

Figure 3: Double cantilever beam: geometry, material data and finite element mesh

is discretized, the rate of the energy refers to the corresponding volume fraction, and thus it must be halved. In contrast to that the symmetry condition in y–direction does not influence μ. In this case the ratio of the energy and the newly opened delamination area remains constant. Thus, the parameter μ is determined via (4) as $\mu = 7.1$. The present analysis is performed controlling the tip displacement. In Fig. 4 the load $\lambda\,qb$ is depicted versus the crack opening displacement w, where w denotes the total mutual tip displacement of the beam. The crack opening process starts when the transverse tensile strength Z_0 is exceeded. In the softening range we notice very good agreement of our results with the experiments, especially for large displacements w. The influence of mesh refinement can be seen for three different meshes with $n_4 = 268, 570, 860$ elements.
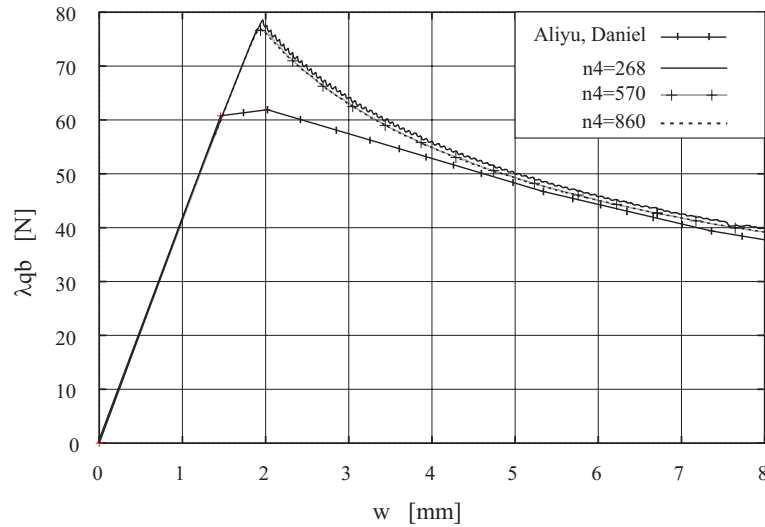

Figure 4: Double cantilever beam, load deflection curves

In Fig. 5 the normal stresses S^{33} are plotted in the x-z-plane for different crack opening displacements. The plots show the concentration of the stresses in front of

the crack tip. The newly opened delamination surface is completely free of stresses.
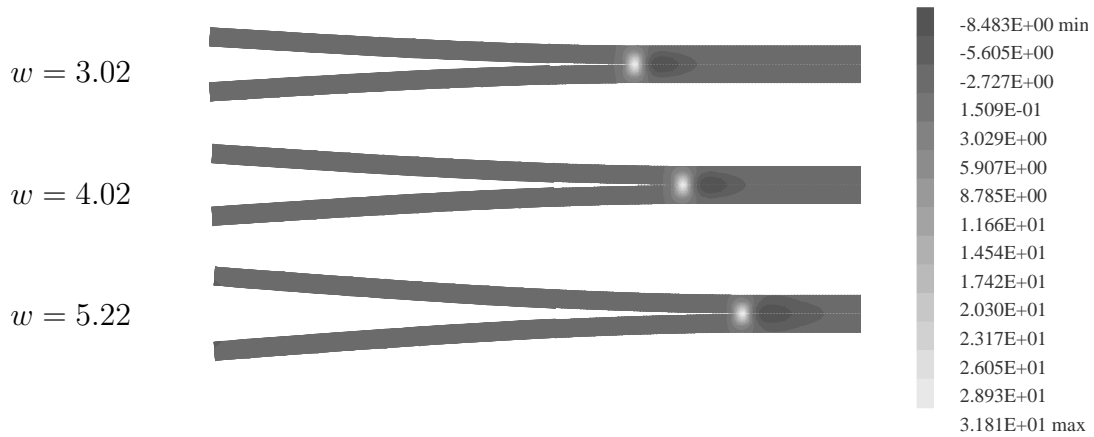

Figure 5: Normal stresses S^{33} in x-z-plane for different crack opening displacements

3.2 Plate with initial circular delamination

The next example is a plate consisting of 16 layers with layer thickness $h_L = 0.12\,mm$, and stacking sequence $[0°/0°/+45°/0°/0°/-45°/0°/90°]_S$. A circular delamination is given between layer 14 and 15, see Fig. 6. Cochelin et.al.[12] investi-
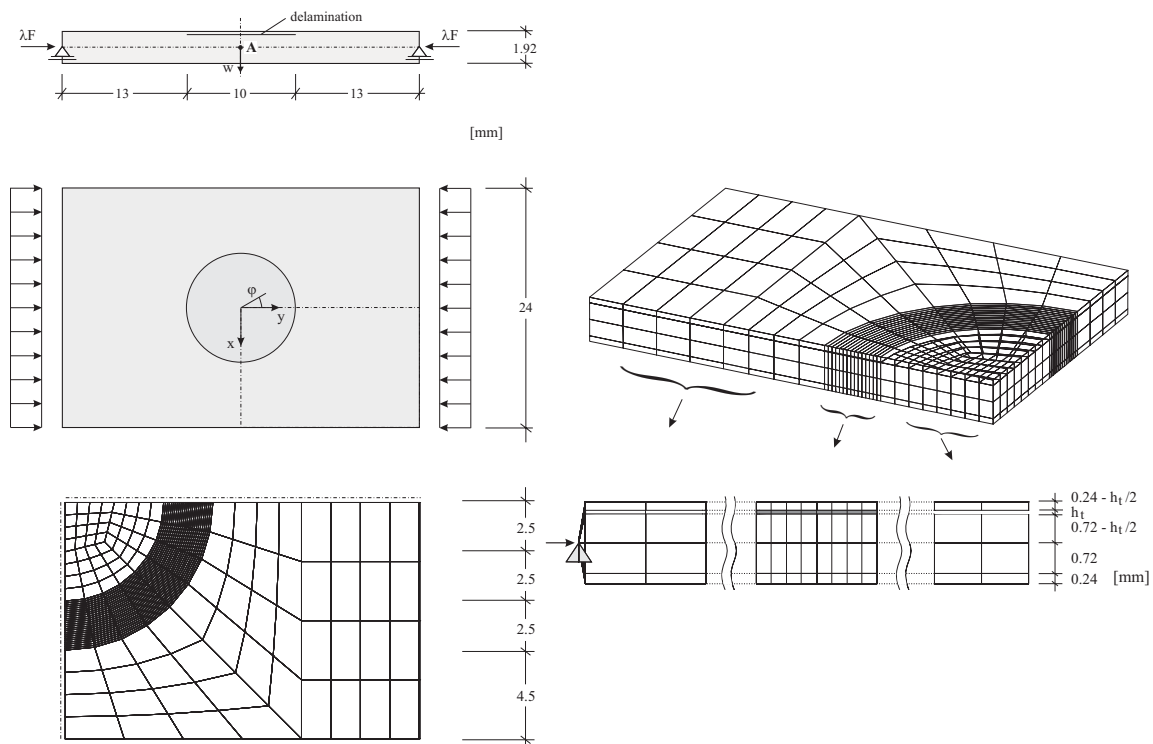

Figure 6: Plate with circular delamination: geometry and finite element mesh

gated the stability behaviour of this structure with nongrowing delaminations. The plate is simply supported along the edges. The geometrical data and the material

data for an AS/3501 graphite epoxy composite are given as follows:

$$
\begin{array}{llllllll}
E_1 & = & 135000 & N/mm^2 & \quad & G_{12} & = & 5150 & N/mm^2 \\
E_2 & = & 8500 & N/mm^2 & \quad & G_{23} & = & 5150 & N/mm^2 \\
\nu_{12} & = & 0.317 & & & & & \\
Z_0 & = & 51.7 & N/mm^2 & \quad & R_0 & = & 91.0 & N/mm^2 \\
h_t & = & 0.005 & mm & \quad & F & = & 30 & N/mm
\end{array}
\tag{15}
$$

Due to the fibre angles with $\pm 45°$ the structure is not symmetric with respect to the x-axis and y–axis, respectively. To reduce the computing effort this fact is ignored in the present analysis. The problem of propagating delaminations can in principle be studied when discretizing only one quarter of the plate, see Fig. 6. The interface elements are positioned between the layers 14 and 15 only in the fine discretized annular space. In thickness direction several physical layers are summarized within one element layer. This has to be considered when performing the numerical integration in thickness direction.[4] The nonlinear calculations are performed controlling the load parameter λ. First, we analyze a "perfect" plate without delamination and thus without the interface layer. Due to the symmetric layup the plate is loaded as a pure membrane. With increasing axial deformation a bifurcation point is found. A switch to the secondary solution path is possible by a perturbation with the first eigenvector. Next, we analyze the behaviour of the plate with artificial and non growing delamination. In this case one obtains a load displacement curve which for large displacements approaches the secondary solution path of the perfect plate. Furthermore the solutions with increasing delamination zone are depicted in Fig. 7. The influence of time step Δt is negligible. Delamination starts at the coordinates $(x = 0\,mm, y = 5\,mm)$ and propagates along the inner circle. The whole process is depicted in Fig. 8.
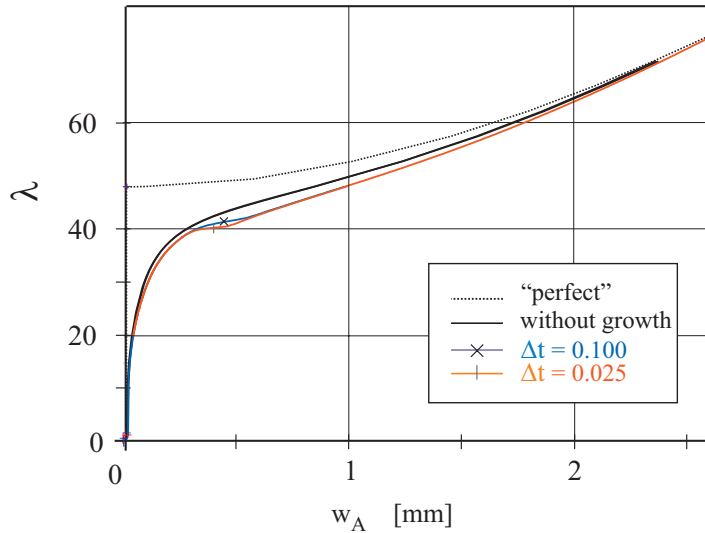

Figure 7: Load deflection curves of the plate

4   CONCLUSIONS

This paper presents a finite element method to simulate increasing delaminations in composite structures. Interface layers are discretized using refined eight–node hexahedrons. These elements have a small, but non–vanishing thickness and are
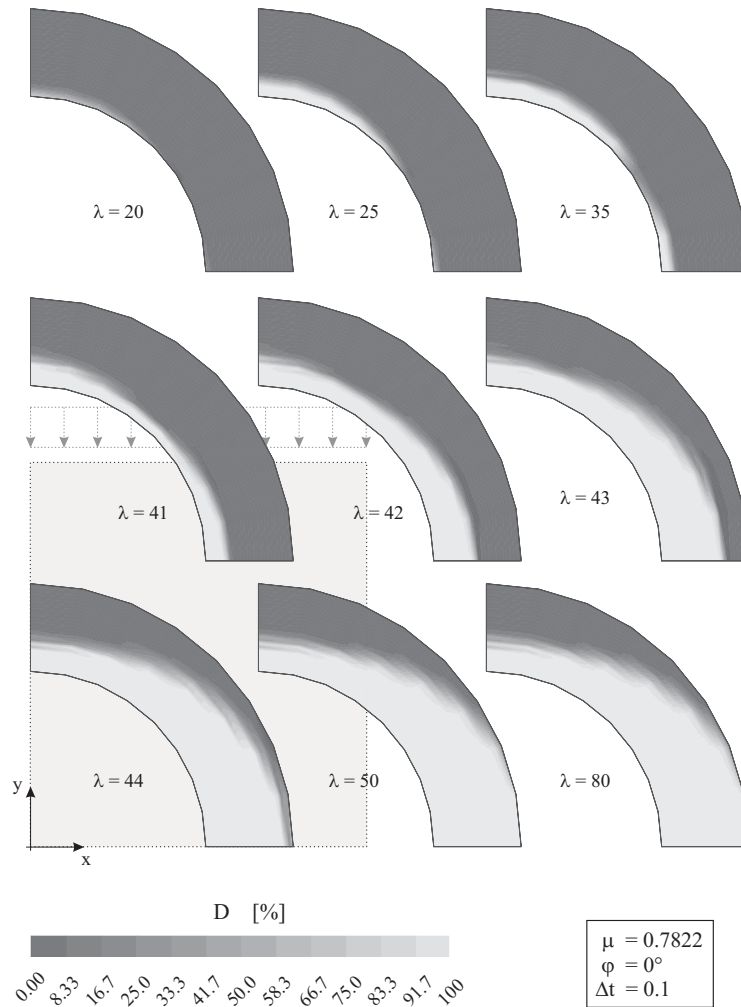
Figure 8: Growing delamination zone

located in those regions where delaminations are expected. Within an inelastic model, the delamination criterion of Hashin is extended to a yield criterion with softening. Numerical instabilities are avoided by a viscoplastic regularization. The viscosity parameter is determined automatically such that the critical energy release rate is the essential material parameter. Detailed numerical calculations show the effectivity, robustness and reliability of the developed delamination model.

REFERENCES

[1] A.S.D. Wang, M. Slomiana, R.B. Bucinell, "Delamination Crack Growth in Composite Laminates", in: Johnson, W.S. (Ed.), *Delamination and Debonding of Materials*, ASTM, 135–167, Philadelphia, 1995.

[2] J.C. Schellekens and R. de Borst, "Free Edge Delamination in Carbon-Epoxy Laminates: A Novel Numerical/Experimental Approach", *Composite Structures,* **28**, 357–373 (1994).

[3] M.A. Crisfield, G. Jelenic, Y. Mi, H.G. Zhong, Z. Fan, "Some Aspects of the Non-linear Finite Element Method", *Finite Elements in Analysis and Design,* **27**, 19–40 (1997).

[4] S. Klinkel, F. Gruttmann, W. Wagner, "A Continuum Based Three-Dimensional Shell Element for Laminated Structures", *Computers & Structures,* **71**, 43–62 (1999).

[5] K.J. Bathe, E. Dvorkin, "A Continuum Mechanics Based Four Node Shell Element for General Nonlinear Analysis", *Engineering Computations,* **1**, 77–88 (1984).

[6] P. Betsch, E. Stein, "An Assumed Strain Approach Avoiding Artificial Thickness Straining for a Nonlinear 4-Node Shell Element", *Communications in Numerical Methods in Engineering,* **11**, 899–910 (1995).

[7] W. Sprenger, F. Gruttmann, W. Wagner, "Delamination growth analysis in laminated structures with continuum based 3D-shell elements and a viscoplastic softening model", *Computer Methods in Applied Mechanics and Engineering,* **185**, 123–139 (2000).

[8] Z. Hashin "Failure Criteria for Unidirectional Composites", *J. Appl. Mech.,* **47**, 329–334 (1980).

[9] G. Duvaut, J.L. Lions, *Les Inequations en Mechanique et en Physique*, Dunod, Paris, (1972).

[10] A.A. Aliyu, I.M. Daniel, "Effects of Strain Rate on Delamination Fracture Toughness of Graphite/Epoxy", in: W.S. Johnson, (Ed), *Delamination and Debonding of Materials, ASTM STP 876*, 336–348, Philadelphia, 1985.

[11] F. Gruttmann, W. Wagner, "On the Numerical Analysis of Local Effects in Composite Structures", *Composite Structures,* **29**, 1–12 (1994).

[12] B. Cochelin, N. Damil, M. Potier-Ferry, "Asymptotic-Numerical Methods and Padé Approximants for Nonlinear-Elastic Structures", *Int. J. Num. Meth. Engng.,* **37**, 1137–1213 (1994).